Proteolytic maturation and activation of autotaxin (NPP2), a secreted metastasis-enhancing lysophospholipase D

Silvia Jansen[1,*], Cristiana Stefan[1,*], John W. M. Creemers[2], Etienne Waelkens[1], Aleyde Van Eynde[1], Willy Stalmans[1] and Mathieu Bollen[1,‡]

[1]Division of Biochemistry and [2]Department for Human Genetics, Flanders Interuniversity Institute for Biotechnology, Faculty of Medicine, K.U.Leuven, B-3000 Leuven, Belgium

*These authors contributed equally to this work

‡Author for correspondence (e-mail: Mathieu.Bollen@med.kuleuven.ac.be)

Accepted 13 April 2005
Journal of Cell Science 118, 3081-3089 Published by The Company of Biologists 2005
doi:10.1242/jcs.02438

Summary

Autotaxin (NPP2) is an extracellular protein that is upregulated in various malignancies, including breast and lung cancer. It potently stimulates cell proliferation, cell motility and angiogenesis, which is accounted for by its intrinsic lysophospholipase-D activity that generates the lipid mediators lysophosphatidic acid and sphingosine-1-phosphate. Based on its structural similarities with the better characterized nucleotide pyrophosphatase/phosphodiesterase NPP1, it has always been assumed that NPP2 is also synthesized as a type-II integral membrane protein and that extracellular NPP2 is generated from this membrane precursor. We show here, however, using domain swapping and mutagenesis experiments as well as N-terminal protein sequencing, that NPP2 is actually synthesized as a pre-pro-enzyme and that the proteolytically processed protein is secreted. Following the removal of a 27-residue signal peptide by the signal peptidase, NPP2 is subsequently cleaved by proprotein convertases (PCs). The removal of an N-terminal octapeptide by PCs is associated with an enhanced activity of NPP2 as a lysophospholipase D. These novel insights in the maturation of NPP2 have also implications for the development of NPP2 inhibitors as potential anti-cancer agents.

Key words: Autotaxin, NPP2, Lysophospholipase D, Furin, Signal peptide

Introduction

Autotaxin, also known as NPP2 (nucleotide pyrophosphatase/phosphodiesterase 2) and hereafter referred to as NPP2] is a protein of 103 kDa that is synthesized by a variety of normal cells and tissues (Bächer et al., 1999; Stefan et al., 1999; Bollen et al., 2000; Ferry et al., 2003). However, its expression is increased in various malignancies, including breast and lung cancer, and this upregulation correlates with the invasiveness of the cancer cells (Kohn et al., 1993; Lee et al., 1996; Kawagoe et al., 1997; Yang et al., 1999; Zhang et al., 1999; Debies and Welch, 2002; Euer et al., 2002; Yang et al., 2002; Kehlen et al., 2004). The expression of NPP2 is also about 100-fold upregulated during transformation by the oncoprotein *v-Jun* (Black et al., 2004). NPP2 is an attractive target for the treatment of cancer because it acts extracellularly and stimulates the metastatic cascade at multiple levels. Indeed, NPP2 not only stimulates the growth of cancer cells (Umezu-Goto et al., 2002), but also acts as a tumour cell motility factor (Kohn et al., 1993; Lee et al., 1996), augments the tumorigenicity of *ras*-transformed cells (Nam et al., 2000) and induces a strong angiogenic response (Nam et al., 2001). All known biological effects of NPP2 can be explained by its ability to act as an extracellular lysophospholipase D (reviewed by Moolenaar, 2002; Moolenaar et al., 2004; Tokumura, 2004; Xie and Meier, 2004). A major substrate of NPP2 is lysophosphatidylcholine (Umezu-Goto et al., 2002; Tokumura et al., 2002; Hama et al., 2004), which is hydrolyzed into lysophosphatidic acid (LPA) and choline. LPA evokes a variety of biological responses via G-protein coupled LPA receptors (Moolenaar et al., 2004). Thus, LPA stimulates: (1) cell proliferation via *ras* activation; (2) cell survival via activation of protein kinase B; (3) cell rounding via activation of the RhoA GTPase; and (4) cell spreading and migration via activation of the Rac GTPase. LPA is also angiogenic by stabilizing endothelial monolayer barriers and by stimulating vascular endothelial growth factor (VEGF) expression. Another substrate of NPP2 is sphingosylphosphorylcholine, which is hydrolysed into sphingosine-1-phosphate and choline (Clair et al., 2003). Sphingosine-1-phosphate is also a modulator of cell motility but its effects are complex and cell-type dependent.

NPP2 is one of seven known members of the nucleotide pyrophosphatase/phosphodiesterase (NPP) family (reviewed by Bollen et al., 2000; Goding et al., 2003; Duan et al., 2003). The NPPs have a structurally related catalytic domain and an identical catalytic mechanism, but they differ in their substrate specificity (Gijsbers et al., 2001; Gijsbers et al., 2003a; Koh et al., 2003). The best-characterized NPP is NPP1, which releases nucleoside 5′-monophosphates from a variety of nucleotides and nucleotide derivatives. For example, NPP1 releases pyrophosphate from ATP, an inhibitor of bone mineralization

Journal of Cell Science

Journal of Cell Science

and tissue calcification (Bollen et al., 2000; Goding et al., 2003). NPP1 is a type-II transmembrane protein that accumulates in the plasma membrane. It contains a short N-terminal cytoplasmic domain that is involved in the targeting of NPP1 to the basolateral membrane (Bello et al., 2001), a single transmembrane domain and a large extracellular domain. The extracellular domain consists consecutively of two somatomedin-B like domains that mediate homodimerization via disulfide bonds, the catalytic domain and a C-terminal nuclease-like domain with an unknown function (Goding et al., 2003; Gijsbers et al., 2003b).

Since NPP1 and NPP2 have a similar domain structure, it has always been assumed that NPP2 is also an integral membrane protein and that the extracellular form originates from proteolysis of the plasma membrane-associated precursor, resulting in the release of an N-terminally nicked polypeptide (Clair et al., 1997; Moolenaar, 2002; Goding et al., 2003). We have analyzed the origin of extracellular NPP2 and, unexpectedly, we have found that NPP1 and NPP2 follow a different trafficking and maturation pathway. NPP2 appears to be synthesized as a pre-pro-enzyme and the removal of the pro-peptide by furin-like proteases is required for its full activation.

Materials and Methods

NPP constructs

The construction of chimaeras of the N-terminal, catalytic and nuclease-like domains of mouse NPP1 and rat NPP2 have been described previously (Cimpean et al., 2004). The same strategy was used to create NPP1 with the N-terminus of NPP2, i.e. $NPP2_{1-35}$-1, and NPP2 with the N-terminus of NPP1, i.e. $NPP1_{35-85}$-2. For this purpose a *Sac*II restriction site was introduced in codon 84-85 and codon 34-35 of full-length NPP1 and NPP2, respectively. After digestion with *Sac*II, the purified NPP1/NPP2 fragments were ligated to generate $NPP2_{1-35}$-1 and $NPP1_{35-85}$-2. For the swapping of the hydrophobic domains of NPP1 and NPP2, a multi-step PCR-strategy was used. A first PCR generated N-terminal fragments of NPP1 and NPP2, i.e. codons 35-58 of NPP1 and codons 1-11 of NPP2, followed by a primer-born 3′ overlap with the hydrophobic domains of NPP2 and NPP1, respectively. These fragments were used as sense primers in the second PCR reaction with NPP2 and NPP1 as templates, respectively, and generated $NPP1_{35-58}$-2 and $NPP2_{1-11}$-1. The products of the second PCR reaction were ligated into a vector and used as template DNA in the next PCR reaction. For this PCR an anti-sense primer was designed that annealed to the last amino acids of the hydrophobic domain of NPP1 or NPP2 and had a non-annealing overlap with the domain following the hydrophobic domain of NPP2 and NPP1 respectively. The fragments generated, i.e. NPP1-(35-58)/NPP2-(12-30)/NPP1-80-87 and NPP2-(1-11)/NPP1-(59-79)/NPP2-(31-38), were purified from the agarose gel and used as sense primers in a PCR with NPP1 and NPP2 as template, respectively. After the PCR reaction, the template DNA mixture was destroyed with *Dpn*I and the DNA fragments were digested with the appropriate restriction enzymes and ligated into a vector containing an N-terminal HA (haemagglutinin)-tag and a C-terminal Myc-tag. The ligation mixture was used to transform the DH5α bacterial strain. EGFP-tagged rat NPP2, used for confocal microscopy, was obtained by *Xba*I and *Bgl*II cleavage of EGFP-N_1 (Clontech) and rat NPP2. The latter was created by PCR using pcDNA3-RnNPP2-myc (donated by J. Aoki) as template and 5′-CTCGAGTCTAGAATGGCAAGA-CAAGGCTGTCTCGGG-3′(containing an *Xba*I site) and 5′-C-CGCGGCAGATCTACAATCTCGCTCTCATATGTATGCAGGTA-3′ (containing a *Bgl*II site) as sense and antisense primers, respectively. Subsequently, both DNA fragments were ligated and used to transform the DH5α bacterial strain. Positives colonies were identified by PCR check-up.

Site-directed mutagenesis of the hydrophobic domain was performed using the QuickChange™ kit (Stratagene). Four amino acids of NPP2 were changed for the corresponding amino acids of NPP1, such that each mutant had an overlap of one amino acid with the previous one. To monitor the cleavage of NPP2 at a specific site, a Flag-tag was inserted after Gly27, Phe28 or Arg35. This was done by PCR with a sense primer starting at Phe28, Thr29 or Ala36 and containing the Flag-tag at its 5′ end, and an antisense primer starting at Gly27, Phe28 or Arg35. After the PCR reaction, the mixture was treated with *DpnI*, phosphorylated and ligated to obtain circular DNA for transformation of DH5α bacteria. All chimaeric and mutated constructs were verified by sequence analysis.

Cell culture and RNA-interference

HEK293 cells were maintained at 37°C under a humidified atmosphere containing 5% CO_2 in Dulbecco's modified Eagle's medium, supplemented with 10% (v/v) heat-inactivated foetal bovine serum, penicillin (100 units/ml) and streptomycin (100 μg/ml). Mouse insulinoma β-TC3 cells were maintained in DMEM F12 medium under the same conditions. Cells were transiently transfected at 30-40% confluency using the Fugene™ 6 transfection system (Roche Diagnostics). The cells were harvested 24-72 hours after transfection, washed once in PBS and lysed in 50 mM Tris/HCl at pH 7.5, 0.5 mM phenylmethanesulphonyl fluoride, 0.5 mM benzamidine, 150 mM NaCl and 1% (v/v) Triton X-100. After ultracentrifugation (45 minutes at 100,000 ***g***), the supernatant (cell lysate) was used for western blot analysis.

For the RNAi-mediated knockdown of furin or PACE4, short hairpin RNAs (shRNAs), consisting of 19 sense and antisense nucleotides separated by a hairpin loop and complementary to the target mRNA, were cloned into the mU6pro-vector (Yu et al., 2002). The targeted sequences were 5′ GACCATTCGACCAAACAGT 3′ and 5′ GCTCTTCATCCAGTTTTGC 3′ for the knockdown of furin and PACE4, respectively. Mouse insulinoma β-TC3 cells were transiently co-transfected with HA-NPP2-Myc with a Flag-tag inserted after Arg35 and an RNAi plasmid, as indicated. The levels of endogenous furin and PACE4 are too low to be detected by immunoblotting. Therefore, as a control for the RNAi, we overexpressed furin and PACE4 in β-TC3 cells and showed that the expression of these proteins was silenced with the respective shRNAs. All cells were harvested 48 hours after transfection and analysed by immunoblotting.

Immunofluorescence

HEK293 cells were seeded in four-well chambers at a density of 30,000 cells/well. Cells were transfected using the Fugene™ 6 transfection agent. After 24 hours, the medium was removed and the cells were washed twice in phosphate-buffered saline (PBS). Cells transfected with NPP2-EGFP were fixed and looked at immediately. For the visualisation of NPP1, the endoplasmic reticulum, the Golgi apparatus and the trans-Golgi network, cells were fixed in 2% formaldehyde during 10 minutes. Subsequently, the cells were permeabilised with 40 μg/ml digitonin for 10 minutes. After washes in PBS, non-specific binding was reduced by washing the cells with 3% bovine serum albumin in PBS for 20 minutes. Following this blocking step, the cells were incubated with anti-Myc (clone 9E10) or anti-Golgin-97 (clone CDF4, Molecular Probes, Invitrogen) anti-BiP (donated by L. Hendershot), anti-TGN38 (Transduction Laboratories, Lexington, KY), anti-γ-adaptin-1 (Sigma) antibodies for 90 minutes. Cells were washed again and incubated for 60 minutes with a secondary antibody, i.e. Alexa Fluor 594 (Molecular Probes, Invitrogen) for fluorescence microscopy and anti-mouse FITC (Sigma) or Alexa Fluor 543 for confocal microscopy. After washing

in PBS, the fluorescence was visualized with an LSM 510 axiovert 100M laser-scanning microscope or an Olympus fluorescence microscope (pictures not shown), as indicated.

Lysophospholipase-D assay and immunoblotting

Lysophospholipase-D assays were done on aliquots of cell lysates, culture medium or purified autotaxin, as described by Gijsbers et al. (Gijsbers et al., 2003a), with slight modifications. Briefly, the substrate lysophosphatidylcholine (14:0) or sphingosylphosphorylcholine was prepared in 12 mM chloroform-methanol (3:1) and stored at –20°C. Before the assay, an aliquot of the substrate was dried with N_2 and reconstituted to 4 mM in 200 mM Tris at pH 9, 10 mM $MgCl_2$, and 10 mM $CaCl_2$. 10 µl of the substrate was mixed with the same volume of sample and incubated at 37°C for 5-60 minutes. Subsequently, the released choline was quantified spectrophotometrically at 540 nm after incubation for 5 minutes with 50 µl of each the peroxidase reagent (50 mM Tris at pH 9.0, 2 mM TOOS, 5 U/ml peroxidase and 0.01% Triton X-100) and the choline oxidase reagent (50 mM Tris at pH 9.0, 2 mM aminoantipyrine, 5 U/ml choline oxidase and 0.01% Triton X-100). The production of choline was linear within the time frame that we adopted and was, because of the high substrate concentration (2 mM) and the limited conversion to product, not hampered by product inhibition (van Meeteren et al., 2005).

Following SDS-PAGE (4-12% Bis-Tris gels of Biorad) and transfer to polyvinylidene fluoride membranes (Amersham) at 100 V in 192 mM glycine, 25 mM Tris and 10% methanol (pH 8.6), non-specific binding sites were blocked with 3% bovine serum albumin (Serva) and 0.1% Tween-20 in PBS, supplemented with 1 mM $CaCl_2$ for the membranes intended for incubation with anti-Flag M1. Blocking of the membranes destined for anti-Flag M2 incubation occurred in 5% (w/v) nonfat powdered milk in PBS plus 0.2% Triton X-100. The membranes were incubated with monoclonal anti-Myc (clone 9E10), anti-HA (clone HA-7), anti-Flag M1 (Sigma Aldrich) and anti-Flag M2 antibodies (Sigma Aldrich), as indicated. After incubation with anti-Myc, anti-HA or anti-Flag M1 antibodies the blots were washed three times in PBS with 0.1% Tween-20, supplemented with 1 mM $CaCl_2$ in case the blot was incubated with anti-Flag M1. Following incubation with anti-Flag M2, washes were performed in PBS with 0.2% Triton X-100. HRP-goat anti-mouse IgG (Dako) was used as a secondary antibody for all primary antibodies. The protein bands were visualised by ECL-treatment of the blot, followed by exposure to Hyperfilm ECL.

Purification and N-terminal sequencing of NPP2 fusions

Hybridoma cells (clone 9E10) were used for the production of anti-c-Myc monoclonal antibodies. Cells were grown in DMEM containing 10% foetal bovine serum, 2 mM glutamine, penicillin 100 U/ml, streptomycin 100 µg/ml and 25 mM glucose. When the cells were 80% confluent the medium was replaced by serum-free medium and the cells were maintained in culture for one additional week. Antibodies were purified from the medium by affinity chromatography on Protein-A Sepharose (Amersham). The purified anti-Myc antibodies were randomly coupled to CNBr-activated Sepharose 4B and the matrix was used for affinity purification of NPP2 fusions with a C-terminal Myc tag. The retained NPP2 fusions were eluted with 0.1 M triethanolamine at pH 12. Following SDS-PAGE and blotting onto a polyvinylidene fluoride membrane (Amersham) the NPP2 fusions were visualized by Amido-black 10B (Biorad) staining and N-terminally sequenced the by Edman degradation.

Results

Mapping of the determinants for the extracellular release of NPP2

NPP1 is an integral plasma membrane protein in a variety of

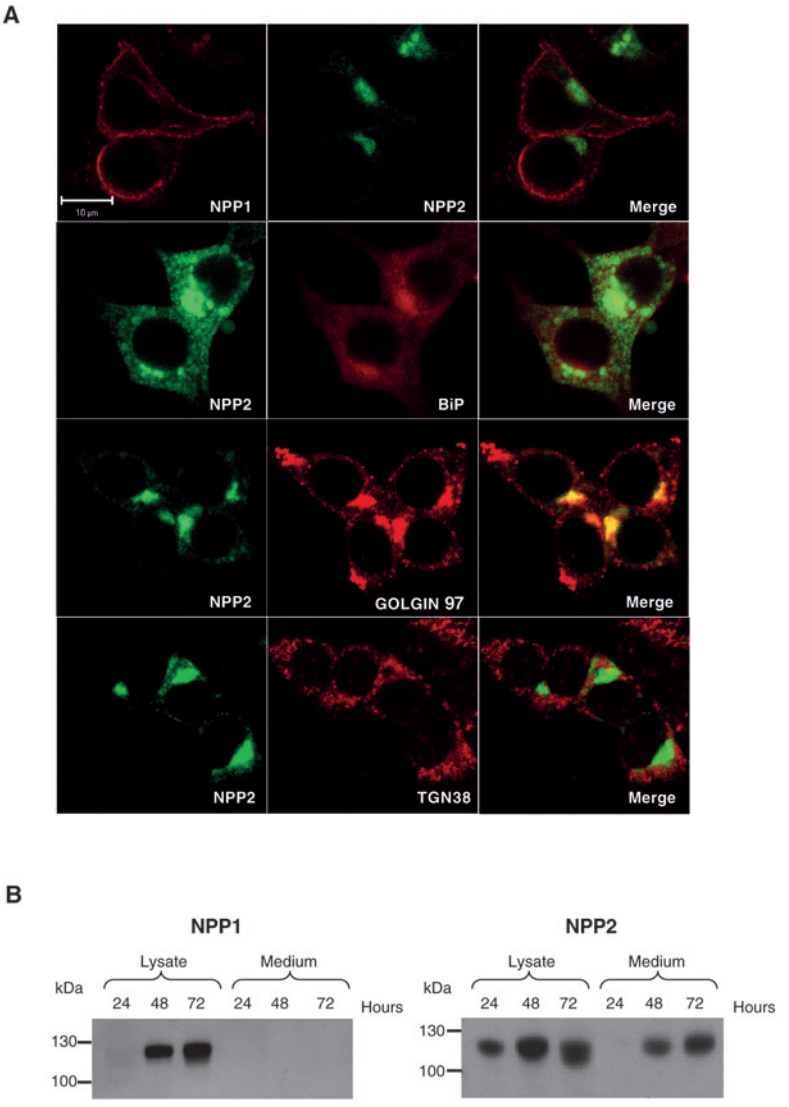

Fig. 1. Localization of NPP1 and NPP2 in HEK293 cells. (A) Cells were transiently transfected with HA-NPP1-Myc and NPP2-EGFP (upper three panels) or with NPP2-EGFP alone (lower nine panels). After 24 hours, the cells were fixed with 2% formaldehyde. NPP2-EGFP, HA-NPP1-Myc, the ER-marker BiP, the Golgi-marker Golgin-97 and the trans-Golgi network marker TGN38 were visualized by confocal microscopy using the spontaneous green fluorescence of EGFP, anti-Myc antibodies, anti-BiP antibodies, anti-TGN38 antibodies or anti-Golgin-97 antibodies, as indicated. The right panels represent the merges of the left and middle panels. (B) HEK293 cells were transiently transfected with HA-NPP1-Myc or HA-NPP2-Myc. At the indicated time points, the fusion proteins were detected by immunoblotting of the cell lysates and the culture medium with anti-Myc antibodies.

cells and tissues (Stefan et al., 1998; Bollen et al., 2000; Goding et al., 2003; Gijsbers et al., 2003b; Vaingankar et al., 2004). When expressed in HEK293 cells, NPP1 was also largely targeted to the cell periphery, as detected by both regular fluorescence (not shown) and confocal fluorescence microscopy (Fig. 1A). Fractionation experiments confirmed that NPP1 was associated with the plasma membrane fraction of HEK293 cells and could be solubilized with Triton X-100 (not shown). NPP2 has always been assumed to display a similar subcellular distribution as NPP1. However, we found that in HEK293 cells NPP2-EGFP (Fig. 1A) as well as HA-NPP2-myc (not shown) displayed a more cytoplasmic distribution than did NPP1. NPP2-EGFP clearly co-localized with a marker for the Golgi apparatus (Golgin-97), but showed little co-localisation with markers for the endoplasmic reticulum (BiP), the trans-Golgi network (TGN38) (Fig. 1A), and the clathrin-coated vesicles of the trans-Golgi network (anti-γ-adaptin) (not shown).

Immunoblotting showed an accumulation of NPP1 in HEK293 cells 48-72 hours after transfection but did not visualize NPP1 in the non-concentrated culture medium (Fig. 1B). By contrast, similar levels of NPP2 were detected in the cell lysates and the non-concentrated culture medium 48-72 hours after transfection. Since the cell volume is small compared to the culture-medium volume, this implies that the large majority of NPP2 was extracellular. Indeed, lysophospholipase-D activity assays revealed that 98.8% of the NPP2 that had been synthesized by 72 hours was present in the culture medium (not illustrated).

To map the protein fragments that are responsible for the different maturation pathways of NPP1 and NPP2, we used a domain-swapping approach (Fig. 2A). Chimaeras of the N-terminal, catalytic and nuclease-like domains of NPP1 and NPP2 were expressed with an N-terminal HA-tag and a C-terminal Myc-tag. All NPP chimaeras with the N-terminal domain of NPP2 were efficiently secreted, whereas the chimaeras with the N-terminus of NPP1 remained cell-associated (Fig. 2B). Swapping of the catalytic and nuclease-like domains did not affect the localization of the resulting chimaeras. Thus, the N-terminal domain emerges as the sole determinant for the targeting of NPP1 and NPP2 to the plasma membrane or the culture medium, respectively. The N-terminal domain of NPP1 and NPP2 consists consecutively of a polar, a hydrophobic and two somatomedin-B-like subdomains (Fig. 2A). Swapping of the hydrophobic subdomain between NPP1 and NPP2, with or without the N-terminal polar subdomain, was sufficient to retarget these isozymes (Fig. 2C). This finding strongly suggests that the hydrophobic subdomain determines the trafficking pathway of NPP1 and NPP2. Finally, we have generated six NPP2 mutants by replacing the residues of the hydrophobic subdomain four by four by the corresponding residues of NPP1 (Fig. 2D). Surprisingly, these mutants accumulated in the medium to a similar extent as did NPP2, suggesting that the targeting of NPP2 is not determined by a sequence motif within its hydrophobic subdomain.

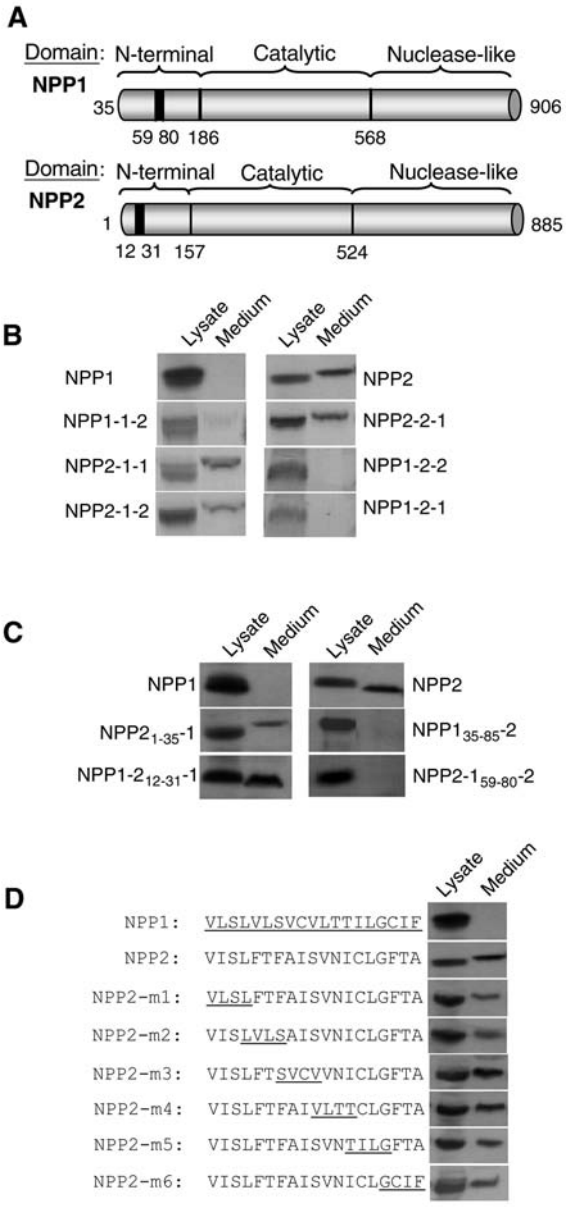

Fig. 2. Mapping of the polypeptide fragment that determines the extracellular release of NPP2.(A) The domain structure of NPP1 and NPP2. The hydrophobic fragment in the N-terminal domain is represented by a thick black vertical line. (B) Secretion by HEK293 cells of NPP1, NPP2 and the indicated chimaeras of the N-terminal, catalytic and nuclease-like domains of NPP1 and NPP2, as defined in panel A. NPP1-1-2 refers to a fusion of the N-terminal and catalytic domains of NPP1 and the nuclease-like domain of NPP2. The other chimaeras are annotated in the same manner. All proteins were expressed with an N-terminal HA-tag and a C-terminal Myc-tag, and were visualized after 72 hours by immunoblotting with anti-Myc antibodies. (C) Extracellular release of NPP1, NPP2 and the indicated chimaeras of the N-terminal subdomains, all expressed for 72 hours with an N-terminal HA-tag and a C-terminal Myc-tag and visualized by immunoblotting with anti-Myc antibodies. NPP1-2_{12-30}-1 refers to NPP1 with its N-terminal hydrophobic subdomain (residues 59-79) swapped for the corresponding subdomain (residues 12-30) of NPP2. The other fusions are annotated in the same manner. (D) Effect of mutation of the N-terminal hydrophobic domain on the secretion of HA-NPP2-Myc. The residues of the hydrophobic domain of NPP2 were replaced four by four by the corresponding residues of NPP1. The secretion of wild-type NPP1, NPP2 and the NPP2 mutants was visualized by immunoblotting with anti-Myc antibodies. All data shown in panels B-D are representative for at least three independent experiments.

NPP1 and NPP2 harbour a signal anchor and signal peptide, respectively

In further agreement with the view that the trafficking pathways of NPP1 and NPP2 are determined by their N-terminal hydrophobic subdomain, we observed that NPP1 with the hydrophobic subdomain of NPP2 (NPP1-$2_{12\text{-}30}$-1) had a subcellular localization similar to that of NPP2 (Fig. 3A). Conversely, NPP2 with the hydrophobic subdomain of NPP1 (NPP2-$1_{59\text{-}79}$-2) was targeted to the plasma membrane. Collectively, our data are consistent with the notion that the hydrophobic subdomain of NPP1 is part of a classical 'signal anchor' that mediates the uptake of NPP1 in the endoplasmic reticulum and that anchors NPP1 as a type-II transmembrane protein. The accumulation of NPP2 and NPP1-$2_{12\text{-}30}$-1 in the medium could then be the result of intramembrane proteolysis, ectodomain shedding or processing of the N-terminal region as a 'signal peptide'. To differentiate between these possibilities we have examined whether there exists a cellular pool of NPP2 with an intact N-terminus, which would be expected to accumulate if NPP2 were solubilized by intramembrane proteolysis or ectodomain shedding during its later stages of maturation. By contrast, if NPP2 were synthesized as a pre-protein, the N-terminal signal peptide would be expected to be removed during translation. In Fig. 3B it is shown that NPP1 and NPP2-$1_{59\text{-}79}$-2 in cell lysates retained HA-immunoreactivity and thus had an intact N-terminus, whereas the N-terminus of NPP2 and NPP1-$2_{12\text{-}30}$-1 lost its N-terminus, in accordance with the view that NPP2 possesses an N-terminal signal peptide.

The Signal-P program (Nielsen et al., 1997) predicts with 99% certainty that the N-terminus of NPP1 functions as a signal anchor (not shown), whereas the N-terminal 27 residues of NPP2 are identified with 93% certainty as a cleavable signal sequence (Fig. 4A). Interestingly, the mutations of the hydrophobic region of NPP2 that are described in Fig. 2D and that did not affect the secretion of NPP2, were also not predicted by the Signal-P program to affect the functionality of the signal sequence. The predicted signal sequence of NPP2 consists of an N-terminal polar region with a net positive charge, a hydrophobic core of 10 residues and a C-terminal polar region with a small residue at position –1 (Gly) and an uncharged residue at position –3 (Cys), all in close accordance with the properties of established signal sequences (Martoglio and Dobberstein, 1998; Stroud and Walter, 1999). To explore whether NPP2 is indeed intracellularly hydrolysed after Gly27, as predicted by the Signal-P program, we made use of anti-Flag antibodies that either recognize the Flag-epitope only when it contains a free aminoterminus (M1-antibody) or that recognize both an N-terminally free as well as an internal Flag-epitope (M2-antibody) (Stroud and Walter, 1999). We generated fusions of NPP2 with a Flag-tag inserted after either Gly27 or Phe28. The M2 antibodies recognized both fusions in the cell lysates and the medium, whereas the M1 antibodies only recognized the fusion with the Flag-tag after Gly27, consistent with the prediction that NPP2 is proteolyzed

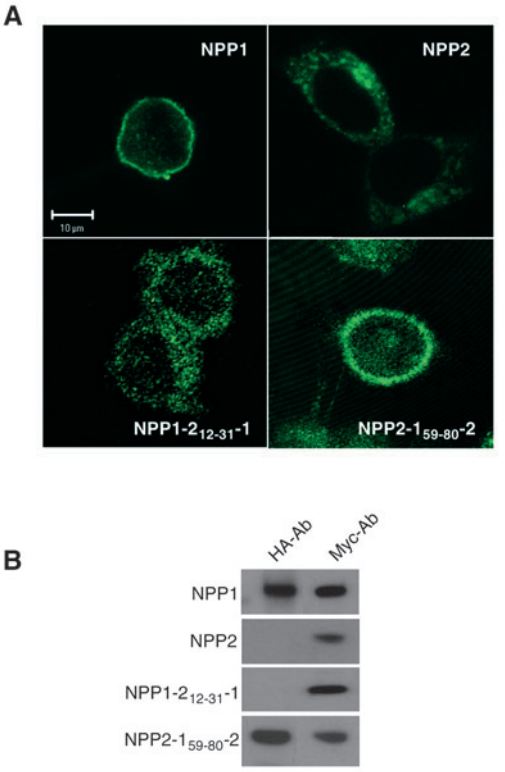

Fig. 3. The hydrophobic subdomain determines the trafficking pathways of NPP1 and NPP2. (A) Localization in HEK293 cells of NPP1, NPP2, NPP1-$2_{12\text{-}30}$-1 and NPP2-$1_{59\text{-}79}$-2, each expressed as fusions with an N-terminal HA-tag and a C-terminal Myc-tag, and detected by confocal fluorescence microscopy with anti-Myc antibodies. (B) An aliquot of the same cells was lysed for immunoblotting with anti-HA and anti-Myc antibodies. All data shown are representative for at least three independent experiments.

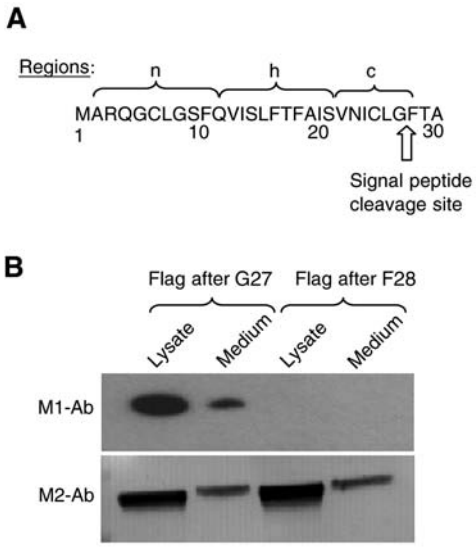

Fig. 4. The N-terminus of NPP2 functions as a signal peptide. (A) The N-terminal sequence of NPP2 with the predicted N-terminal (n), hydrophobic (h) and C-terminal (c) fragment of the signal peptide sequence, as predicted by the Signal P program (version 3.1). Also indicated is the predicted cleavage site (arrow). (B) HA-NPP2-Myc, with a Flag epitope inserted after either Gly27 or Phe28, was expressed in HEK 293 cells. 24 hours after transfection the cells were harvested and the lysates were subjected to immunoblotting with anti-Flag M1 and M2 monoclonal antibodies. The M1 antibodies only recognize an N-terminally free Flag-tag, whereas the M2s also recognize an internal Flag-tag. The data are representative for at least three independent experiments.

after Gly27 (Fig. 4). As a further support for this conclusion, we expressed HA-NPP2-Myc in HEK293 cells, affinity-purified the NPP2 fusion from the cell lysates after 24 hours and identified by N-terminal sequencing Phe28 of NPP2 as the first residue (not illustrated). Following the removal of the pre-peptide, pre-proteins follow the classical secretory pathway. That this also holds true for NPP2 is indicated by our observation (not illustrated) that the accumulation of NPP2 in the culture medium was largely abolished by brefeldin A, an inhibitor of protein transport from the endoplasmic reticulum to the Golgi apparatus (Klausner et al., 1992).

NPP2 is also processed by proprotein convertases

C-terminal to the signal peptidase cleavage site, NPP2 contains the sequence (residues 32-35) Arg-Ile-Lys-Arg (Fig. 5A), a consensus site for cleavage by furin and other members of the family of proprotein convertases (PCs) (Thomas, 2002; Taylor et al., 2003; Duckert et al., 2004). To examine whether NPP2 is indeed processed by PCs, we introduced a Flag epitope after Arg35. Immunoblotting with M1 and M2 antibodies confirmed that NPP2 was cleaved after Arg35, both intracellularly and in the medium (Fig. 5B). However, the M1/M2 signal ratio was much higher in the medium than in the cell lysate, indicating that proteolysis between Arg35 and Ala36 only occurred just before or after secretion. Cleavage of pro-NPP2 was not detectably affected by the addition of a cell-impermeable inhibitor (0.1 mM hexa-D-arginine) of furin(-like) endoproteases to the culture medium (Cameron et al., 2000), indicating that processing by furins occurred either primarily intracellularly or by a PC that is insensitive to hexa-D-arginine (not illustrated). Conversely, the proteolysis between Arg35 and Ala36, as detected with the M1 antibodies, was blocked by the co-expression of α_1-antitrypsin Portland (α_1-PDX) (Fig. 5C), which inhibits most PCs under these conditions (Jean et al., 1998; Benjannet et al., 1997). Moreover, following the RNAi-mediated knockdown of furin or PACE4 in mouse insulinoma β-TC3 cells, the removal of the pro-peptide was hampered (Fig. 5D). Cleavage of NPP2 between Arg35 and Ala36 could also be confirmed by N-terminal sequencing of NPP2 that was affinity-purified from the medium (not shown). Moreover, NPP2 that was affinity-purified from the culture medium after the co-expression with α1-PDX started with Phe28, the first residue after hydrolysis by the signal peptidase.

Surprisingly, after mutation of the residues that conform to the furin consensus site (residues 32-35) into an alanine, NPP2 in the medium still started with Ala36. At first glance this could be taken as evidence that this motif is not required for hydrolysis by PCs. However, the Signal-P program predicted with 94% certainty that these mutations changed the hydrolysis site of the signal peptidase from that after Gly27 to that after Ala35 (Arg35 in the wild type), which is topologically equivalent to the PC cleavage site.

Comparison of pro-NPP2 and NPP2

The expression of HA-NPP2-Myc in the presence or absence of α1-PDX enabled us to compare the properties of pro-NPP2 and NPP2. Neither immunoblotting (Fig. 6A) nor pulse-chase experiments (not shown) provided any evidence for different rates of synthesis, secretion and turnover of pro-NPP2 and NPP2. However, affinity-purified NPP2 consistently showed a 30% higher specific lysophospholipase-D activity than did pro-NPP2, assayed with either lysophosphatidylcholine (Fig. 6B) or sphingosylphosphorylcholine (not shown) as substrates. We have

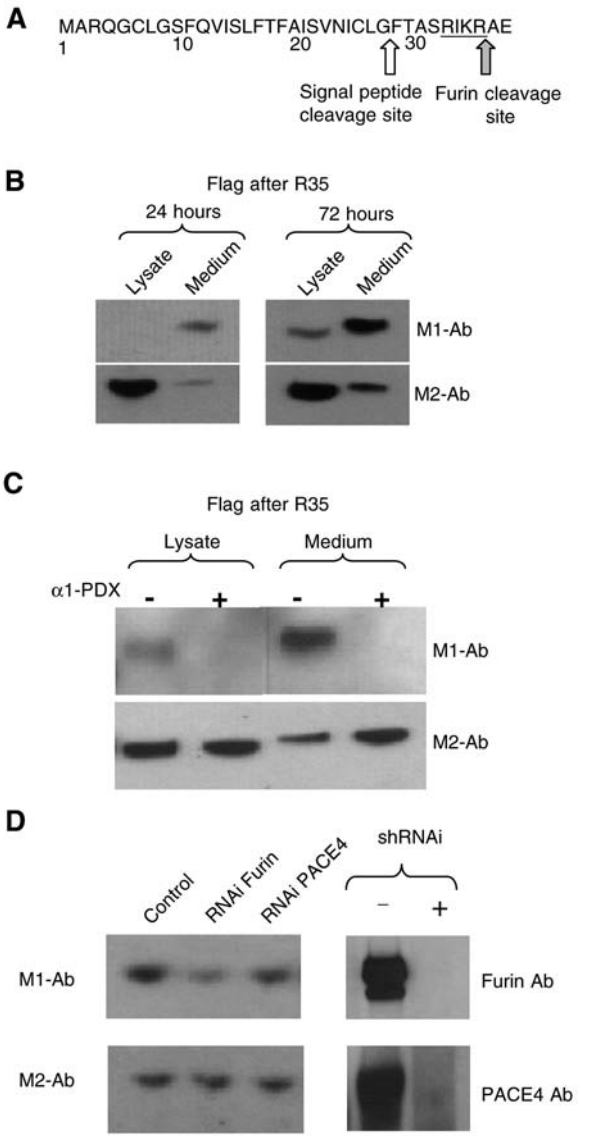

Fig. 5. NPP2 is processed by furin-like endoproteinases. (A) The N-terminal sequence of NPP2 with the predicted signal peptide cleavage site (white arrow), the consensus site for recognition by furin (underlined) and the predicted furin cleavage site (grey arrow). (B) HA-NPP2-Myc with the Flag-tag inserted after Arg35 was expressed in HEK293 cells. After 24 hours and 72 hours the cell lysates and culture medium were processed for immunoblotting with the anti-Flag M1 and M2 monoclonal antibodies. (C) The same NPP2 construct was also expressed for 72 hours with or without the furin-inhibitor α_1-PDX, and the corresponding lysates and media were immunoblotted with the M1 and M2 antibodies. (D) HA-NPP2-Myc with a Flag-tag after Arg35 was expressed in β-TC3 cells before or after the RNAi-mediated knockdown of furin or PACE4, as indicated. Aliquots of the culture medium were processed for immunoblotting with the M1 and M2 antibodies. The right panels show the effect of the furin or PACE4 shRNAs on the level of overexpressed furin or PACE4, respectively, as detected by immunoblotting. The data are representative for at least three independent experiments.

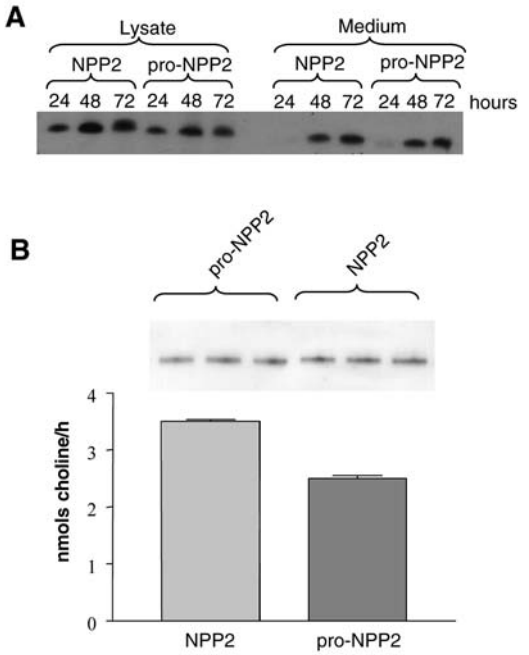

Fig. 6. Comparison of pro-NPP2 and NPP2. (A) HA-NPP2-Myc was expressed in HEK293 cells with or without the furin-inhibitor α_1-PDX, to generate pro-NPP2 and NPP2, respectively. After 24 hours, 48 hours and 72 hours the cell lysates and culture media were processed for immunoblotting with anti-Myc antibodies. (B) Pro-NPP2 and NPP2, obtained after the expression of HA-NPP2-Myc with or without the furin-inhibitor α_1-PDX, respectively, were purified on an anti-Myc affinity column. The purified enzymes were assayed for lysophospholipase-D activities. The bar diagrams represent the means ±s.e.m. (n=3) of the enzymatic activities. Pro-NPP2 and NPP2 were assayed at the same concentration, as measured in triplicate by immunoblotting with anti-c-Myc antibodies (inset).

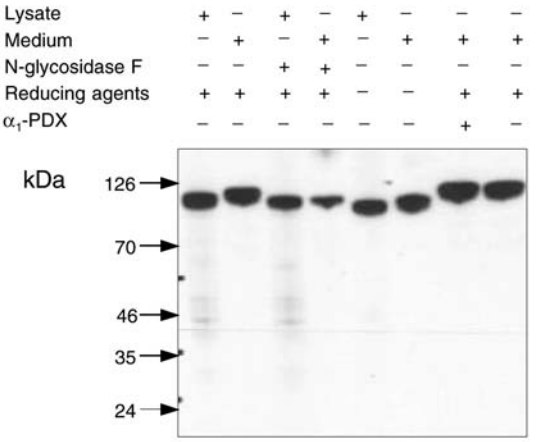

Fig. 7. Cellular and secreted NPP2 differ in their extent of glycosylation. HA-NPP2-Myc was expressed in HEK293 cells with or without α_1-PDX, as indicated. The cell lysates and media were processed for immunoblotting with anti-Myc antibodies in the absence or presence of 50 mM 2-mercaptoethanol and before or after a pretreatment for 50 mU of *N*-glycosidase F, as indicated. The data are representative for at least three independent experiments.

also considered the possibility that the pro-peptide is secreted together with NPP2 and regulates its catalytic activity. However, up to 10 μM of the synthetic pro-peptide (FTASRIKR) did not affect the lysophospholipase-D activity of NPP2 (not shown). Moreover, neither the pre-peptide nor the pro-peptide could be detected by immunofluorescence microscopy with antibodies against the N-terminal HA-tag or Flag-tag, respectively (not shown), indicating that these peptides are rapidly targeted for degradation and do not have an additional biological function.

Secreted and cell-associated NPP2 are differently glycosylated

Compared with the cell-associated pool of NPP2, secreted NPP2 consistently migrated slower during SDS-PAGE (Fig. 2, Fig. 5B, Fig. 7). This difference cannot be explained by the removal of the pro-peptide since pro-NPP2, if anything, migrated slower than NPP2 (Fig. 7, last two lanes; see also Fig. 6). Neither did the distinct migration of cell-associated and secreted NPP2 reflect a different sensitivity to reducing agents, since their mobility remained distinct in the absence of reducing agents. However, after a pretreatment of the cellular and secreted pool of NPP2 with N-glycosidase F they migrated identically, showing that the composition of their N-linked oligosaccharides is different.

Tokumura et al. previously speculated that NPP2 is a heterodimer of full-length NPP2 and a C-terminal 30-kDa fragment, roughly corresponding to the nuclease-like domain (Tokumura, 2004; Tokumura et al., 2002). However, we did not detect lower-molecular-mass bands in crude or purified preparations of NPP2 with antibodies against the C-terminal Myc-tag.

Discussion

At first glance, NPP2 has the same domain structure as NPP1 and NPP3, two established integral plasma membrane glycoproteins with a type-II orientation (Bollen et al., 2000; Goding et al., 2003; Duan et al., 2003). For this reason, NPP2 was also widely believed to be synthesized as a type-II transmembrane protein. However, our data unequivocally show that NPP2 does not accumulate in the plasma membrane (Fig. 1A and Fig. 3) and is synthesized as a pre-pro-enzyme. Indeed, the N-terminus of NPP2 conforms to a consensus signal sequence (Fig. 4A) and cleavage of the signal peptide was confirmed by N-terminal sequencing of the cell-associated NPP2 as well as by immunoblotting with M1 and M2 antibodies that can differentiate between an internal and an N-terminally free Flag-epitope that was inserted just after the predicted cleavage site (Fig. 4B). Importantly, NPP1 with the signal peptide of NPP2 was also secreted (Fig. 2C), suggesting that there are no additional determinants for secretion. The N-terminus of pro-NPP2 contains a consensus cleavage site for PCs (Fig. 5) and the occurrence of this cleavage was confirmed by N-terminal sequencing of secreted NPP2 and by the use of the anti-Flag epitope M1 and M2 antibodies (Fig. 5C). Moreover, processing of the pro-peptide was inhibited by the co-expression of the furin inhibitor α_1-PDX (Fig. 5B), a genetically engineered serpin that inhibits most PCs under these conditions, and by the RNAi-mediated knockdown of furin or PACE4 (Fig. 5D). In further agreement with the processing of NPP2 as a pre-pro-protein via a secretory

Journal of Cell Science

pathway, we found that NPP2 co-localized with a marker of the Golgi-apparatus (Fig. 1A), and that its secretion was inhibited by brefeldin A, an inhibitor of protein transport from the endoplasmic reticulum to the Golgi apparatus. In the current study we have only examined the processing of NPP2 in HEK293 cells but it seems likely that NPP2 is processed identically in vivo since the first residue of NPP2 from human plasma was Ala36 (Tokumura et al., 2000), which is also the first residue of NPP2 after processing by PCs.

We have found that cleavage of pro-NPP2 by PCs is associated with a moderate activation of NPP2 as a lysophospholipase-D (Fig. 6B), similar to the activation of BACE, the β-secretase involved in the processing of the amyloid precursor protein (Benjannet et al., 2001; Creemers et al., 2001). However, the removal of the pro-peptide does not appear to play a role in the secretion or stability of NPP2 since an inhibition of cleavage by furins did not affect the extracellular accumulation of NPP2 (Fig. 6A). In further agreement with this view we found that NPP1 with the signal peptide of NPP2, but lacking the pro-peptide of NPP2, was also efficiently secreted (Fig. 2C). PCs belong to the seven member family of subtilisin-like proprotein convertases that are implicated in the proteolysis and activation of a variety of substrates including neuropeptides, peptide hormones, growth factors, enzymes, coagulation factors, viral coat proteins and bacterial toxins. Furin is expressed in all cells and represents the workhorse of the family but most cell types also express other isozymes that have (partially) overlapping substrate specificity (Thomas, 2002; Taylor et al., 2003). Our data suggest that pro-NPP2 is a substrate not only for furin but also for at least one other isozyme, namely PACE4 (Fig. 5D).

NPP2 is an attractive target for the treatment of cancer because it acts extracellularly and promotes tumour development at various levels (see Introduction). In principle, inhibitors of NPP2 function could be directed towards its synthesis, maturation and/or its catalytic activity. One feasible target would be the inhibition of NPP2 processing by PCs. Interestingly, PCs themselves have been implicated in tumorigenesis, and clinical trials with furin inhibitors as an anticancer treatment are underway (Thomas, 2002; Taylor et al., 2003). It is possible that the efficiency of furin-inhibitors as anticancer agents stems, at least in part, from their effect on the maturation of NPP2. Conversely, our current work suggests that the inhibition of maturation of NPP2 with furin inhibitors would only moderately decrease the lysophospholipase-D activity of NPP2. Therefore, the development of inhibitors of the transcription or the catalytic activity of NPP2 emerges as a more attractive therapeutic goal.

This work was supported by the Fund for Scientific Research – Flanders (grant G.0082.02). Silvia Jansen is a Research Assistant of the Fund for Scientific Research – Flanders. John Creemers is a postdoctoral fellow of the Fund for Scientific Research – Flanders. Suzy Hermans, Sandra Meulemans and Karen Schildermans are acknowledged for excellent technical assistance

References

Bächner, D., Ahrens, M., Betat, N., Schröder, D. and Gross, G. (1999). Developmental expression analysis of murine autotaxin (ATX). *Mech. Dev.* **84**, 121-125.

Bello, V., Goding, J. W., Greengrass, V., Sali, A., Dubljevic, V., Lenoir, C., Trugnan, G. and Maurice, M. (2001). Characterization of di-leucine-based signal in the cytoplasmic tail of the nucleotide-pyrophosphatase NPP1 that mediates basolateral targetting but not endocytosis. *Mol. Biol. Cell* **12**, 3004-3015.

Benjannet, S., Savaria, D., Laslop, A., Munzer, J. S., Chretien, M., Marcinkiewicz, M. and Seidah, N. G. (1997). Alpha1-antitrypsin Portland inhibits processing of precursors mediated by proprotein convertases primarily within the constitutive secretory pathway. *J. Biol. Chem.* **272**, 26210-26218.

Benjannet, S., Elagoz, A., Wickam, L., Mamarbachi, M., Munzer, J. S., Basak, A., Lazure, C., Cromlish, J. A., Sisodia, S., Checler, F. et al. (2001). Post-translational processing of beta-secretase (beta-amyloid-converting enzyme) and its ectodomain shedding. The pro- and transmembrane/cytosolic domains affect its cellular activity and amyloid-beta production. *J. Biol. Chem.* **276**, 10879-10887.

Black, E., Clair, T., Delrow, J., Neiman, P. and Gillespie, D. (2004). Microarray analysis identifies autotaxin, a tumour cell motility and angiogenic factor with lysophospholipase D activity, as a specific target of cell transformation by v-Jun. *Oncogene* **23**, 2357-2366.

Bollen, M., Gijsbers, R., Ceulemans, H., Stalmans, W. and Stefan, C. (2000). Nucleotide pyrophosphatases/phosphodiesterases on the move. *Crit. Rev. Biochem. Mol. Biol.* **35**, 393-432.

Cameron, A., Appel, J., Hougthen, R. A. and Lindberg, I. (2000). Polyarginines are potent furin inhibitors. *J. Biol. Chem.* **275**, 36741-36749.

Cimpean, A., Stefan, C., Gijsbers, R., Stalmans, W. and Bollen, M. (2004). Substrate-specifying determinants of the nucleotide pyrophosphatases/phosphodiesterases NPP1 and NPP2. *Biochem. J.* **381**, 71-77.

Clair, T., Lee, H., Liotta, L. A. and Stracke, M. (1997). Autotaxin is an exoenzyme possessing 5′-nucleotide phosphodiesterase/ATP pyrophosphatase and ATPase activities. *J. Biol. Chem.* **272**, 996-1001.

Clair, T., Aoki, J., Koh, E., Bandle, R. W., Nam, W., Ptaszynska, M. M., Mills, G. B., Schiffmann, E., Liotta, L. A. and Stracke, M. (2003). Autotaxin hydrolyzes sphingosylphosphorylcholine to produce the regulator of migration, sphingosine-1-phosphate. *Cancer Res.* **63**, 5446-5453.

Creemers, J. W., Ines Dominguez, D., Plets, E., Serneels, L., Taylor, N. A., Multhaup, G., Craessaerts, W. and De Strooper, B. (2001). Processing of beta-secretase by furin and other members of the proprotein convertases. *J. Biol. Chem.* **276**, 4211-4217.

Debies, M. and Welch, D. (2002). Genetic basis of human breast cancer metastasis. *J. Mammary Gland Biol.* **6**, 441-451.

Duan, R., Bergman, T., Xu, N., Wu, J., Cheng, Y., Duan, J., Nelander, S., Palmberg, C. and Nilsson, A. (2003). Identification of human intestinal alkaline sphingomyelinase as a novel ecto-enzyme related to the nucleotide phosphodiesterase family. *J. Biol. Chem.* **278**, 38528-38536.

Duckert, P., Brunak, S. and Blom, N. (2004). Prediction of proprotein convertase cleavage sites. *Protein Eng. Des. Sel.* **17**, 107-112.

Euer, N., Schwirzke, M., Evtimova, V., Burtscher, H., Jarsch, M., Tarin, D. and Weidle, U. (2002). Identification of genes associated with metastasis of mammary carcinoma in metastatic versus non-metastatic cell lines. *Anticancer Res.* **22**, 733-740.

Ferry, G., Telliers, E., Try, A., Grés, S., Naime, I., Simon, M. F., Rodriguez, M., Bouchez, J., Tack, I., Gesta, S. et al. (2003). Autotaxin is released from adipocytes, catalyzes lysophosphatidic acid synthesis, and activates preadipocyte proliferation. *J. Biol. Chem.* **278**, 18162-18169.

Gijsbers, R., Ceulemans, C., Stalmans, W. and Bollen, M. (2001). Structural and catalytic similarities between nucleotide pyrophosphatases/phosphodiesterases and alkaline phosphatases. *J. Biol. Chem.* **276**, 1362-1368.

Gijsbers, R., Aoki, J., Arai, H. and Bollen, M. (2003a). The hydrolysis of lysophopholipids and nucleotides by autotaxin (NPP2) involves a single catalytic site. *FEBS Lett.* **538**, 60-64.

Gijsbers, R., Ceulemans, H. and Bollen, M. (2003b). Functional characterization of the non-catalytic ectodomains of the nucleotide pyrophosphatase/ phosphodiesterase NPP1. *Biochem. J.* **371**, 321-330.

Goding, J. W., Grobben, B. and Slegers, H. (2003). Physiological and pathophysiological functions of the ecto-nucleotide pyrophosphatase/phospodiesterase family. *Biochim. Biophys. Acta* **1638**, 1-19.

Hama, K., Aoki, J., Fukaya, M., Kishi, Y., Sakai, T., Suzuki, R., Ohta, H., Yamori, T., Watanabe, M., Chun, J. et al. (2004). Lysophosphatidic acid and autotaxin stimumate cell motility of neoplastic and non-neoplastic cells through LPA_1. *J. Biol. Chem.* **279**, 17634-17639.

Jean, F., Stella, K., Thomas, L., Liu, G., Xiang, Y., Reason, A. J. and Thomas, G. (1998). α_1-Antitrypsin Portland, a bioengineered serpin highly

selective for furin: Application as an antipathogenic agent. *Proc. Natl. Acad. Sci. USA* **95**, 7293-7298.

Kawagoe, H., Stracke, M., Nakamura, H. and Sano, K. (1997). Expression and transcriptional regulation of the PD-I?/autotaxin gene in neuroblastoma. *Cancer Res.* **57**, 2516-2521.

Kehlen, A., Englert, N., Seifert, A., Klonisch, T., Dralle, H., Langner, J. and Hoang-Vu, C. (2004). Expression, regulation and function of autotaxin in thyroid carcinomas. *Int. J. Cancer* **109**, 833-838.

Klausner, R. D., Donaldson, J. G. and Lippincott-Schwartz, J. Brefeldin A: Insights into the control of membrane traffic and organelle structure. *J. Cell Biol.* **116**, 1071-1080.

Kohn, E. C., Hollister, G. H., DiPersio, J. D., Wahl, S., Liotta, L. A. and Schiffmann, E. (1993). Granulocyte-macrophage colony-stimulating factor induces human melanoma-cell migration. *Int. J. Cancer* **53**, 968-972.

Kohn, E., Clair, T., Woodhouse, E., Schiffmann, E., Liotta, L. A. and Stracke, M. (2003). Site-directed mutations in the tumor-associated cytokine, autotaxin, eliminate nucleotide phosphodiesterase, lysophospholipase D and motogenic activities. *Cancer Res.* **63**, 2042-2045.

Lee, H. Y., Murata, J., Clair, T., Polymeropoulos, M. H., Torres, R., Manrow, R. E., Liotta, L. A. and Stracke, M. (1996). Cloning, chromosomal localization, and tissue expression of autotaxin from human teratocarcinoma cells. *Biochem. Biophys. Res. Commun.* **218**, 714-719.

Martoglio, B. and Dobberstein, B. (1998). Signal sequences: more than just greasy peptides. *Trends Cell Biol.* **8**, 410-415.

Moolenaar, W. (2002). Lysophospholipids in the limelight: autotaxin takes the center stage. *J. Cell Biol.* **158**, 197-199.

Moolenaar, W., van Meeteren, L. and Giepmans, B. (2004). The ins and outs of lysophosphatidic acid signaling. *BioEssays* **26**, 870-881.

Nam, S., Clair, T., Campo, C., Lee, H., Liotta, L. A. and Stracke, M. (2000). Autotaxin (ATX), a potent tumor motogen, augments invasive and metastatic potential of *ras*-transformed cells. *Oncogene* **19**, 241-247.

Nam, S., Clair, T., Kim, Y., McMarlin, A., Schiffmann, E., Liotta, L. A. and Stracke, M. (2001). Autotaxin (NPP-2), a metastasis enhancing motogen, is an angiogenic factor. *Cancer Res.* **61**, 6938-6944.

Nielsen, H., Engelbrecht, J., Brunak, S. and Von Heijne, G. (1997). Identification of prokaryotic and eukaryotic signal peptides and prediction of their cleavage sites. *Protein Eng.* **10**, 1-6.

Stefan, C., Stalmans, W. and Bollen, M. (1998). Growth-related expression of the ectonucleotide pyrophosphatase PC-1 in rat liver. *Hepatology* **28**, 1497-1503.

Stroud, R. M. and Walter, P. (1999). Signal sequence recognition and protein targetting. *Curr. Opin. Struct. Biol.* **9**, 754-759.

Taylor, N. A., Van de ven, W. J. M. and Creemers, J. W. M. (2003). Curbing activation: proprotein convertases in homeostasis and pathology. *FASEB J.* **17**, 1215-1227.

Thomas, G. (2002). Furin at the cutting edge: from protein traffic to embryogenesis and disease. *Nat. Rev. Mol. Cell. Biol.* **3**, 753-766.

Tokumura, A. (2004). Metabolic pathways and physiological and pathological significances of lysolipid phosphate mediators. *J. Cell. Biochem.* **92**, 869-881.

Tokumura, A., Majima, E., Kariya, Y., Tominaga, K., Kogure, K., Yasuda, K. and Fukuzawa, K. (2002). Identification of human plasma lysophospholipase D, a lysophosphatidic acid-producing enzyme, as autotaxin, a multifunctional phosphodiesterase. *J. Biol. Chem.* **277**, 39436-39442.

Umezu-Goto, M., Kishi, Y., Taira, A., Hama, K., Dohmae, N., Takio, K., Yamori, T., Mills, G., Inoue, K., Aoki, J. et al. (2002). Autotaxin has lysophospholipase D activity leading to tumor cell growth and motility by lysophosphatidic acid production. *J. Cell Biol.* **158**, 227-233.

Vaingankar, S. M., Fitzpatrick, T. A., Johnson, K., Goding, J. W. and Terkeltaub, R. (2004). Subcellular targetting and function of osteoblast nucleotide pyrophosphatase phosphodiesterase 1. *Am. J. Physiol. Cell. Physiol.* **286**, C1177-C1187.

van Meeteren, L. A., Ruurs, P., Christodoulou, E., Goding, J. W., Takakusa, H., Kikuchi, K., Nagano, T. and Moolenaar, W. H. (2005). Inhibition of autotaxin by lysophosphatidic acid and sphingosine-1-phosphate. *J. Biol. Chem.* **280**, 21155-21161.

Xie, Y. and Meier, K. E. (2004). Lysophospholipase D and its role in LPA production. *Cell Signal.* **16**, 975-981.

Yang, S., Lee, J., Park, C., Kim, S., Hong, S., Chung, H., Min, S., Han, J., Lee, H. W. and Lee, H. Y. (2002). Expression of autotaxin (NPP-2) is closely linked to invasiveness of breast cancer cells. *Clin. Exp. Metastas.* **19**, 603-608.

Yang, Y., Mou, L., Liu, N. and Tsao, M. (1999). Autotaxin expression in non-small-cell lung cancer. *Am. J. Respir. Cell. Mol. Biol.* **21**, 216-222.

Yu, J., DeRuiter, S. and Turner, D. (2002). RNA interference by expression of short-interfering RNAs and hairpin RNAs in mammalian cells. *Proc. Natl. Acad. Sci. USA* **99**, 6047-6052.

Zhang, G., Zhao, Z., Xu, S., Ni, L. and Wang, X. (1999). Expression of autotaxin mRNA in human hepatocellular carcinoma. *Chin. Med. J.* **112**, 330-332.

Journal of Cell Science